Adaptive evolution of a rock-paper-scissors sequence along a direct line of descent

Sean W. Buskirk, Alecia B. Rokes, Gregory I. Lang*

Department of Biological Sciences, Lehigh University, Bethlehem PA 18015.

*Correspondence to glang@lehigh.edu

Non-transitivity – commonly illustrated by the rock-paper-scissors game – is purported to be common in evolution despite a lack of examples of non-transitive interactions arising along a single line of descent. We identify a non-transitive evolutionary sequence in the context of yeast experimental evolution in which a 1,000-generation evolved clone loses in direct competition with its ancestor. We show that non-transitivity arises due to the combined effects of adaptation mediated by the evolving nuclear genome combined with the stepwise deterioration of an intracellular virus. We show that multilevel selection is widespread: nearly half of all populations fix adaptive mutations in both the nuclear and viral genomes, and clonal interference and genetic hitchhiking occur at both levels. Surprisingly, we find no evidence that viral mutations increase the fitness of their host. Instead, the evolutionary success of evolved viral variants results from their selective advantage over viral competitors within the context of individual cells. Overall, our results show that widespread multilevel selection is capable of producing complex evolutionary dynamics – including non-transitivity – under simple laboratory conditions.

A common misconception is that evolution is a linear "march of progress," where each genotype along a line of decent is more fit than all those that came before (*1*). Rejecting this misconception implies that evolution is non-transitive and evolutionary succession will, on occasion, produce organisms that are less fit compared to a distant ancestor. In ecology, nontransitive interactions are well-documented in response to resource (*2*) or interference competition (*3*). Early studies in experimental evolution have suggested that non-transitive interactions can arise (*4*); however, little is known regarding how specific

events along a single evolutionary line of descent can lead to non-transitivity. Here we determine the sequence of events leading to the evolution of non-transitivity in a single yeast population during a 1,000-generation evolution experiment. We show that non-transitivity arises through multilevel selection involving both the yeast nuclear genome and the population of a vertically-transmitted virus. By expanding our study of host-virus genome evolution to over 100 additional yeast populations, we find that multilevel selection, and thus the potential for the evolution of non-transitive interactions, is widespread.

Previously we evolved ~600 haploid populations of yeast asexually for 1,000 generations in rich glucose medium (*5*). We characterized extensively the nuclear basis of adaptation for a subset of these populations through whole-genome whole-population time-course sequencing (*6*) and/or fitness quantification of individual mutations (*7*). For one population (BYS1-D08) we isolated individual clones from Generation 0 (Early), Generation 335 (Intermediate), and Generation 1,000 (Late) and performed pairwise competition experiments at multiple starting frequencies (Fig. 1A, detailed methods are available in the supplementary materials). We find that the Intermediate clone is 3.8% more fit relative to the Early clone and that the Late clone is 1.2% more fit relative to the Intermediate clone (Fig 1B). The expectation, assuming additivity, is that the Late clone will be more fit than the Early clone, by roughly 5.0%. Surprisingly, we find that the Late clone is less fit than expected, to the extent that it often loses in pairwise competition with the Early clone (Fig 1B). This fitness disadvantage can be overcome if the Late clone is started at high frequency relative to the early clone (Fig. S1), thus creating a bi-stable system where, above a certain frequency, the Late clone wins but below this frequency it loses.

In a metagenomic analysis of the nuclear mutations previously detected in the evolved yeast populations (*6*), we observe a statistical enrichment in the gene ontology biological process of β-glucan biosynthesis (6.01-fold enrichment, $P<0.0001$). β-glucans are a major component of the yeast cell wall and the primary receptor of the K1 killer toxin secreted by many yeast strains as a mechanism of interference competition (*8*). A prior study reported that many genes, when deleted, confer resistance to the K1 toxin. We observe a statistical enrichment for mutations in genes associated with high levels of

killer toxin resistance (*9*): of the 714 protein-coding mutations dispersed across 548 genes, 40 occur within 11 genes (of 36) that, when deleted, confer a high level of resistance (χ^2=18.4, *df*=1, *P*=1.8x10^{-5}). Nearly all mutations in these toxin resistance genes are nonsynonymous (18 nonsense/frameshift, 21 missense, 1 synonymous), a strong indication of positive selection. These data suggest that the nuclear genomes evolve in response to selective pressure imposed by the presence of the K1 killer toxin.

In *S. cerevisiae*, killer toxins are encoded by non-infectious, double-stranded RNA mycoviruses called killer viruses. Immunity to the toxin is afforded by the pre-processed version of the toxin, forcing yeast cells to maintain the virus for protection. Together, killing ability and immunity comprise the killer phenotype. Using a well-described halo assay (*10*), we find that the ancestral strain of our evolved populations exhibits the killer phenotype: it inhibits growth of a nearby sensitive strain and resists killing by a known killer strain (Fig. S2). By RT-PCR and sequencing we find that our ancestral strain (which was derived from the common lab strain W303-1a) contains the M1-type killer virus (encoding the K1-type killer toxin) with only minor differences from previously sequenced strains (Fig. S3). In the ancestor we also detect the L-A helper virus, which supplies the RNA-dependent RNA polymerase and capsid protein necessary for the killer virus to complete its life cycle.

We asked if the observed non-transitivity in the BYS1-D08 lineage could be explained by evolution of the killer phenotype. Phenotyping of the isolated clones revealed that the Intermediate clone no longer exhibits killing ability and that the Late clone possesses neither killing ability nor immunity (Fig. S4). Killer toxin has been shown to impart frequency dependent selection in structured environments (*11*) and we hypothesized that a stepwise loss of the killer phenotypes was responsible for the frequency-dependent and non-transitive interaction between Early and Late clones. To determine if the presence of killer virus in the early clone is necessary for the evolution of non-transitivity, we cured the Early clone and found that the Late clone was 4.3% more fit than the killer-cured Early clone, with no correlation between fitness and frequency (Fig. 1B) showing that the presence of killer virus in the Early clone is necessary for frequency-dependence and non-transitivity. To determine if viral evolution alone is

sufficient to account for the observed fitness gains in non-transitive interactions, we transferred the killer virus from the Intermediate clone to the cured Early clone and assayed fitness relative to the Early clone (Fig. 1B). We find that the evolved killer virus confers no significant effect on host fitness. Therefore, changes to the killer virus alone are not sufficient to account for the adaptive evolution of non-transitivity in this population, which must involve changes to both the host and viral genomes.

To determine the extent of killer phenotype evolution across all populations, we assayed the killer phenotype of 142 populations that were founded by a single ancestor and propagated at the same bottleneck size as BYS1-D08 (*6*). We find that approximately half of all populations exhibit a loss or weakening of killing ability by Generation 1,000, and ~10% of populations exhibit neither killing ability nor immunity (Fig. 2A, Fig. 2B). We did not observe loss of immunity without loss of killing ability, an increase in killing ability or immunity, or reappearance of killing ability or immunity once it was lost from a population (Fig. S5). Several populations (i.e. BYS2-B09 and BYS2-B12) lost both killing ability and immunity simultaneously, suggesting that a single event can cause the loss of both the killer phenotypes.

Next, we sought to elucidate the genetic basis of changes to the killer phenotypes. We sequenced viral genomes from a subset of yeast populations (n=67) at Generation 1,000, 57 of which change killer phenotype and 10 control populations that retained the ancestral killer phenotypes. Viral genomes isolated from populations that lost killing ability possess 1-3 mutations in the M1 coding sequence – most being missense variants (Fig. 2C). In contrast, only a single synonymous mutation was detected in M1 across the 10 control populations that retained the killer phenotype (χ^2=59.3, *df*=1, *P*=1.4x10^{-13}). The correlation between the presence of mutations in the viral genome and the loss of killing ability is strong evidence that viral mutations are responsible for the changes in killer phenotypes. We estimate that by Generation 1,000 half of all populations have fixed viral variants that alter killer phenotypes (for comparison, *IRA1*, the most common nuclear target, fixes in ~25% of populations).

Of the 57 populations that lost killing ability, 42 fixed one of three single nucleotide polymorphisms, resulting in amino acid substitutions D106G, D253N, and I292M and observed 13, 14, and 15 times, respectively. Given their prevalence, these polymorphisms likely existed at low frequency in the shared ancestral culture (indeed, we detect one of the common polymorphisms, D106G, in individual clones at the Early time point). In addition to the three ancestral polymorphisms, we detect 34 putative *de novo* point mutations that arose during the evolution of individual populations (Table S1). Mutations are localized to the K1 coding sequence, scattered across the four encoded subunits, and skewed towards missense mutations relative to nonsense or frameshift (Fig. 2D). Fourteen of the seventy-eight identified mutations are predicted to fall at or near sites of protease cleavage or post-translational modification necessary for toxin maturation. Overall, however, the K1 coding sequence appears to be under balancing selection (dN/dS=0.90), indicating that certain amino acid substitutions (e.g. those that eliminate immunity but retain killing ability) are not tolerated. In addition, substitutions are extremely biased toward transitions over transversions (Table S2, R=6.4, χ^2=44.2, df=1, P<0.0001), a bias that is also present in other laboratory-derived M1 variants (R=4.1) (*12*) and natural variation of the helper L-A virus (R=3.0) (*13*, *14*). The transition:transversion bias appears specific to viral genomes as the ratio is much lower within evolved nuclear genomes (R=0.8), especially in genes inferred to be under selection (R=0.5) (*6*, *15*, *16*).

Though point mutations are the most common form of evolved variation, we also detected two viral genomes in which large portions of the K1 ORF are deleted (Fig. 2E). Despite the loss of the majority of the K1 coding sequence, the deletion mutants maintain regions of the viral genome necessary for replication and packaging (*17*, *18*). Notably, the two populations that possess these deletion mutants also possess full-length viral variants. The deletion mutants we observe are similar to the ScV-S defective interfering particles that have been shown to outcompete full-length virus due to their decreased replication time (*19*–*21*).

To compare the dynamics of viral genome evolution, nuclear genome evolution, and phenotypic evolution we performed time-course sequencing of viral genomes from three yeast populations that lost killing ability and for which we have whole-population, whole-genome, time-course sequencing data for the nuclear genome (*6*). As with the evolutionary dynamics of the host genome (*6*), the dynamics of viral genome evolution feature clonal interference (competition between mutant genotypes), genetic hitchhiking (an increase in frequency of an allele due to genetic linkage to a beneficial mutation), and sequential sweeps (Fig. 3, Fig. S6). Interestingly, viral sweeps often coincide with nuclear sweeps. Since the coinciding nuclear sweeps often contain known driver mutations, it is possible that the viral variants themselves are not driving adaptation but instead hitchhiking on the back of beneficial nuclear mutations. This is consistent with the observation that the introduction of the viral variant from the Intermediate clone did not affect the fitness of the Early clone (Fig. 1B)

To determine if the loss of killer phenotype is caused solely by mutations in the killer virus, we transferred the ancestral virus and five evolved viral variants to a virus-cured ancestor via cytoduction. Of the five viral variants one exhibited weak killing ability and full immunity (D253N), three exhibited no killing ability and full immunity (P47S, D106G, I292M), and one exhibited neither killing ability nor immunity (-1 frameshift). For each viral variant, the killer phenotype of the cytoductant matched the killer phenotype of the population of origin demonstrating that viral mutations are sufficient to explain changes in killer phenotype (Fig. S7). To determine if any viral variants affect host fitness, we competed all five cytoductants against the ancestor or a virus-cured ancestor. In pairwise competitions in which both competitors shared either killing ability or immunity, no viral variants impacted host fitness; therefore, production of active toxin or maintenance of the virus has no fitness cost to the host (Fig. 4A). In contrast, an incompatibility in the killer phenotype – produced by the simultaneous loss of both killing ability and immunity – results in frequency dependent fitness interactions in the host population. These pairwise competitions show that a stepwise degradation of the killer virus is a neutral process and no evidence that

host fitness is driving the loss of killer phenotype. These findings support previous theoretical and empirical studies (*22*, *23*) that claim that mycoviruses and their hosts have co-evolved to minimize cost.

Since the reconstructed viral variants have no measurable effect on host fitness, we hypothesized that the evolved viral variants may have a selective advantage within the viral population of individual yeast cells. A within-cell advantage has been invoked to explain the invasion of internal deletion variants (e.g. ScV-S (*20*)) but has not been extended to point mutations. To test evolved viral variants for a within-cell fitness advantage, we generated a heteroplasmic diploid strain by mating the ancestor with a haploid cytoductant containing either the I292M (K^-T^+) or -1 frameshift (K^-T^-) viral variant and propagated the heteroplasmic diploids for 8 days with daily single-cell bottlenecks to minimize among-cell selection. We find that killing ability was lost from all lines, suggesting that the evolved viral variants outcompeted the ancestral variant (Fig. 4B). Indeed, sequencing of the intracellular competitions revealed that the viral variant fixed in most lines (Fig. 4C). In some lines, however, the viral variant increased initially before decreasing late. Further investigation into one of these lines revealed that the decrease in frequency of the viral variant corresponded to the sweep of a *de novo* G131D variant (Fig. 4C, inset). Viral variants therefore are constantly arising, and the evolutionary success of the observed variants results from their selective advantage over viral competitors within the context of an individual cell.

We show that host-virus coevolution is widespread – most yeast populations fix nuclear and viral variants by Generation 1,000. We observe complex dynamics such as genetic hitchhiking and clonal interference in the host populations and within the intracellular viral populations. We show that adaptive evolution is non-transitive – organisms will occasionally lose when competed directly against a distant ancestor. We determine the specific genetic events that lead to non-transitivity in one focal population. Overall, our results demonstrate that adaptive evolution is capable of giving rise to non-transitive interactions along an evolutionary lineage, even under simple laboratory conditions.

Materials and Methods

Strains and Growth Conditions

Unless specified otherwise, yeast strains were propagated in YPD (yeast extract, peptone, dextrose) at 30°C. The ancestor and evolved populations were described previously (*5*).

Viral RNA Isolation, cDNA Synthesis, PCR

Nucleic acids were isolated by phenol-chloroform extraction and precipitated in ethanol. Isolated RNA was reverse-transcribed into cDNA using ProtoScript II First Strand cDNA Synthesis Kit (NEB) with either the enclosed Random Primer Mix or the M1-specific oligo M1_R3.

Sanger Sequencing and Bioinformatics Analyses

PCR was performed on cDNA using Q5 High-Fidelity Polymerase (NEB). The K1 ORF was amplified using primers M1_F1 or M1_F5 and M1_R6 (Table S3). The M1 region downstream of the polyA stretch was amplified using M1_F7 and M1_R3. The LA virus was amplified using LA_F2 and LA_R2, LA_F2 and LA_R3, or LA_F3 and LA_R6. PCR products were Sanger sequenced by Genscript.

Mutations were identified and peak height quantified using 4Peaks (nucleobytes). For intracellular competitions, mutation frequency was quantified by both Sanger and Illumina sequencing (see below), with both methods producing nearly identical results (Fig. S8).

The Sanger sequencing data was aligned to publicly-available M1 and LA references (GenBank Accession Numbers U78817 and J04692, respectively) using ApE (A plasmid Editor). The ancestral M1 and LA viruses differed from the references at 7 sites (including 3 K1 missense mutations) and 19 sites, respectively (Fig. S3).

Illumina Sequencing and Bioinformatics Analyses

Multiplexed libraries were prepared using a two-step PCR. First, cDNA was amplified by Q5 High-Fidelity Polymerase (NEB) for 10 cycles using primers I292M_read1 and I292M_read2 or

frameshift_read1 and frameshift_read2 to incorporate a random 8 bp barcode and sequencing primer binding sites. The resulting amplicons were further amplified by Q5 PCR for 15 cycles using primers i5_adapter and i7_adapter to incorporate the sequencing adaptors and indices. Libraries were sequenced on a NovaSeq 6000 (Illumina) at the Genomics Core Facility at Princeton University.

Raw FASTQ files were demultiplexed using a dual-index barcode splitter (*24*) and trimmed using Trimmomatic (*25*) with default settings for paired-end reads. Mutation frequencies were determined by counting the number of reads that contain the ancestral or evolved allele (mutation flanked by five nucleotides).

Halo Assay

Killer phenotype was measured using a high-throughput version of the standard halo assay (*26*) and a liquid handler (BioMek FX). Assays were performed on YPD agar that had been buffered to pH 4.5 (citrate-phosphate buffer) and dyed with methylene blue (0.003%).

Killing ability was assayed against a sensitive tester strain that evolved from the ancestor (unpublished experiment). The sensitive tester was grown to saturation, diluted, and spread onto a 1-well agar plate. Query strains were grown to saturation, concentrated 5x, and spotted on top of the absorbed lawn.

Immunity was assayed against the ancestral strain (killer tester). Query strains were grown to saturation, diluted, and spotted onto a 1-well agar plate. The killer tester was grown to saturation, concentrated 5x, and spotted on top of the absorbed query strain. Plates were incubated at room temperature for 2-3 days before assessment. Killer phenotype was scored according to the scale in shown in Fig. 2.

Strain Construction

The ancestral strain was cured of the M1 and LA viruses by streaking to single colonies on YPD agar and confirmed by halo assay, PCR, and sequencing. A cured ancestral reference was constructed by placing a constitutively expressed fluorescent marker (pACT1-ymCitrine) at the *CAN1* locus in the cured ancestral background. Evolved clones were isolated from population BYS1-D08 at Generations 315 and 1,000 and fluorescently-marked in the same manner.

Karyogamy mutants were constructed by introduction of the *kar1Δ15* allele by two-step gene replacement in the cured a MATα version of the ancestor. The *kar1Δ15*-containing plasmid pMR1593 (gifted by Mark Rose) was linearized with BglII prior to transformation and selection on -Ura. Mitotic excision of the integrated plasmid was selected for plating on 5-fluorotic acid (5-FOA). Next, we performed allele replacement of NatMX with KanMX for selection during viral transfer.

Viral Transfer

Viruses were transferred to MAT**a** strains using the MATα karyogamy mutant as an intermediate. Viral donors (MAT**a**, *ura3*, NatMX) were first transformed with the pRS426 (*URA3*, 2μ ORI) for future indication of viral transfer. Cytoduction was performed by mixing a viral donor with the karyogamy mutant recipient (MATα, *ura3*, KanMX) at a 5:1 ratio on solid media. After a 6 hr incubation at 30°C, the cells were plated on media containing G418 to select for cells with the donor nucleus. Recipients that grew on -Ura (indicator of cytoplasmic mixing) and failed to grow on ClonNat (absence of donor nuclei) then served as donors for the next cytoduction. These karyogamy mutant donors (MATα, *URA3*, KanMX) were mixed with the selected recipient (MAT**a**, *ura3*, NatMX) at a 5:1 ratio on solid media. After a 6 hr incubation at 30°C, the cells were plated on media containing ClonNat to select for cells with donor nuclei. Recipients that grew on -Ura (indicator of cytoplasmic mixing) and failed to grow on ClonNat (absence of the donor nucleus) were then cured of the indicator plasmid by selection on 5-FOA. Killer phenotype was confirmed by halo assays and the presence of the viral variants in the recipient was verified by Sanger sequencing.

Fitness Assays

Competitive fitness assays were performed as described previously (*5*, *6*). To investigate frequency dependence, competitors were mixed at various ratios at the initiation of the experiment. Competitions were performed for 50 generations under conditions identical to the evolution experiment (*5*). Every 10 generations, competitions were diluted 1:1,000 in fresh media and an aliquot was sampled by BD FACS Canto II flow cytometer. Flow cytometry data was analyzed using FlowJo 10.3. Relative fitness was calculated as the slope of the change in the natural log ratio between the experimental and reference strain. To detect frequency dependence, each 10-generation interval was analyzed independently to calculate starting frequency and fitness.

Intracellular Competitions

Within-cell viral competitions were performed by propagating a heteroplasmic diploid and monitoring killer phenotype and viral variant frequency. Diploids were generated by crossing the ancestor with a cytoductant harboring either the I292M or -1 frameshift viral variant. For each viral variant, three diploid lines (each initiated by a unique mating event) were passaged every other day on buffered YPD media for a total of 7 single-cell bottlenecks to minimize among-cell selection. A portion of each transferred colony was cryopreserved in 15% glycerol. Cryosamples were revived, assayed for killer phenotype, and harvested for RNA. Following RT-PCR, samples were sent for Sanger sequencing and Illumina sequencing.

Acknowledgments: We thank Reed Wickner, Amber Rice, and members of the Lang Lab for their comments on the manuscript. **Funding:** This work was supported by the NIH grant 1R01GM127420. **Author contributions:** Conceptualization and writing were performed by SWB and GIL. Investigation was performed by SWB and ABR. **Competing interests:** Authors declare no competing interests. **Data and materials availability:** Illumina data of viral competitions and evolved nuclear genomes are accessible under the BioProject ID PRJNA553562 and PRJNA205542, respectively.

References:

1. S. J. Gould, *Wonderful Life: The Burgess Shale and the Nature of History* (W. W. Norton & Co., New York, 1989).

2. B. Sinervo, C. M. Lively, The rock–paper–scissors game and the evolution of alternative male strategies. *Nature*. **380**, 240–243 (1996).

3. B. C. Kirkup, M. A. Riley, Antibiotic-mediated antagonism leads to a bacterial game of rock–paper–scissors in vivo. *Nature*. **428**, 412–414 (2004).

4. C. E. Paquin, J. Adams, Relative fitness can decrease in evolving asexual populations of *S. cerevisiae*. *Nature*. **306**, 368–371 (1983).

5. G. I. Lang, D. Botstein, M. M. Desai, Genetic variation and the fate of beneficial mutations in asexual populations. *Genetics*. **188**, 647–61 (2011).

6. G. I. Lang *et al.*, Pervasive genetic hitchhiking and clonal interference in forty evolving yeast populations. *Nature*. **500**, 571–574 (2013).

7. S. W. Buskirk, R. E. Peace, G. I. Lang, Hitchhiking and epistasis give rise to cohort dynamics in adapting populations. *Proc. Natl. Acad. Sci. U. S. A.* **114**, 8330–8335 (2017).

8. M. D. Pieczynska, J. A. G. M. de Visser, R. Korona, Incidence of symbiotic dsRNA 'killer' viruses in wild and domesticated yeast. *FEMS Yeast Res.* **13**, 856–859 (2013).

9. N. Pagé *et al.*, A *Saccharomyces cerevisiae* genome-wide mutant screen for altered sensitivity to K1 killer toxin. *Genetics*. **163**, 875–94 (2003).

10. D. R. Woods, E. A. Bevan, Studies on the Nature of the Killer Factor Produced by *Saccharomyces cerevisiae*. *J. Gen. Microbiol.* **51**, 115–126 (1968).

11. D. Greig, M. Travisano, Density-Dependent Effects on Allelopathic Interactions in Yeast.

Evolution (N. Y). **62**, 521–527 (2008).

12. G. Suzuki, J. S. Weissman, M. Tanaka, [KIL-d] Protein Element Confers Antiviral Activity via Catastrophic Viral Mutagenesis. *Mol. Cell.* **60**, 651–660 (2015).

13. M. E. Diamond *et al.*, Overlapping genes in a yeast double-stranded RNA virus. *J. Virol.* **63**, 3983–90 (1989).

14. T. Icho, R. B. Wickner, The double-stranded RNA genome of yeast virus L-A encodes its own putative RNA polymerase by fusing two open reading frames. *J. Biol. Chem.* **264**, 6716–23 (1989).

15. K. J. Fisher, S. W. Buskirk, R. C. Vignogna, D. A. Marad, G. I. Lang, Adaptive genome duplication affects patterns of molecular evolution in *Saccharomyces cerevisiae*. *PLOS Genet.* **14**, e1007396 (2018).

16. D. A. Marad, S. W. Buskirk, G. I. Lang, Altered access to beneficial mutations slows adaptation and biases fixed mutations in diploids. *Nat. Ecol. Evol.* **2**, 882–889 (2018).

17. J. C. Ribas, R. B. Wickner, RNA-dependent RNA polymerase consensus sequence of the L-A double-stranded RNA virus: definition of essential domains. *Proc. Natl. Acad. Sci. U. S. A.* **89**, 2185–9 (1992).

18. J. C. Ribas, T. Fujimura, R. B. Wickner, Essential RNA binding and packaging domains of the Gag-Pol fusion protein of the L-A double-stranded RNA virus of *Saccharomyces cerevisiae*. *J. Biol. Chem.* **269**, 28420–8 (1994).

19. R. Esteban, R. B. Wickner, A deletion mutant of L-A double-stranded RNA replicates like M1 double-stranded RNA. *J. Virol.* **62**, 1278–85 (1988).

20. W. P. Kane, D. F. Pietras, J. A. Bruenn, Evolution of defective-interfering double-stranded RNAs of the yeast killer virus. *J. Virol.* **32**, 692–6 (1979).

21. S. P. Ridley, R. B. Wickner, Defective Interference in the Killer System of *Saccharomyces cerevisiae*. *J. Virol.* **45**, 800–12 (1983).

22. M. D. Pieczynska, D. Wloch-Salamon, R. Korona, J. A. G. M. de Visser, Rapid multiple-level coevolution in experimental populations of yeast killer and nonkiller strains. *Evolution (N. Y).* **70**, 1342–1353 (2016).

23. M. D. Pieczynska, R. Korona, J. A. G. M. De Visser, Experimental tests of host-virus coevolution in natural killer yeast strains. *J. Evol. Biol.* **30**, 773–781 (2017).

24. R. Leach, L. Parsons, barcode_splitter.py (2017), (available at https://bitbucket.org/princeton_genomics/barcode_splitter).

25. A. M. Bolger, M. Lohse, B. Usadel, Trimmomatic: A flexible trimmer for Illumina sequence data. *Bioinformatics*. **30**, 2114–2120 (2014).

26. A. Crabtree *et al.*, A Rapid Method for Sequencing Double-Stranded RNAs Purified from Yeasts and the Identification of a Potent K1 Killer Toxin Isolated from *Saccharomyces cerevisiae*. *Viruses*. **11**, 70 (2019).

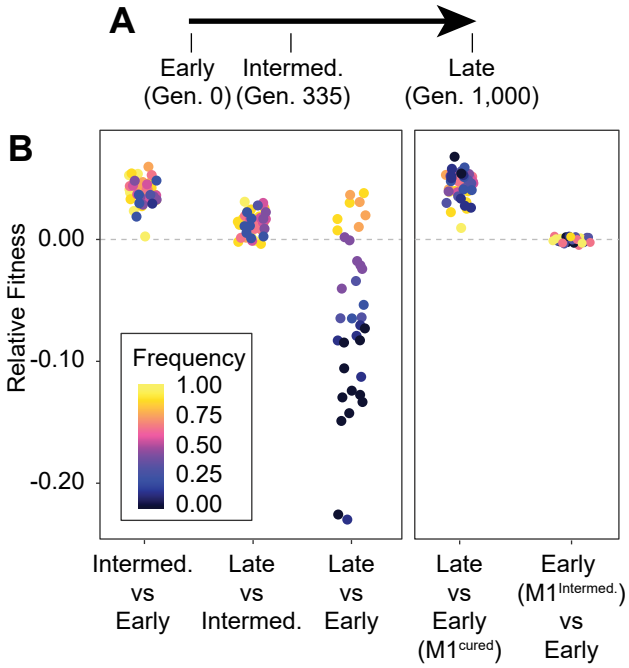

Fig. 1. Non-transitivity and positive frequency dependence arise along an evolutionary lineage. Left: Relative fitness of Early (Gen. 0), Intermediate (Gen. 335), and Late (Gen. 1,000) clones. Right: Relative fitness of the Early clone without ancestral virus or with the viral variant from the Intermediate clone. Fitness and starting frequency correspond to the later clone relative to the earlier clone during pairwise competitions.

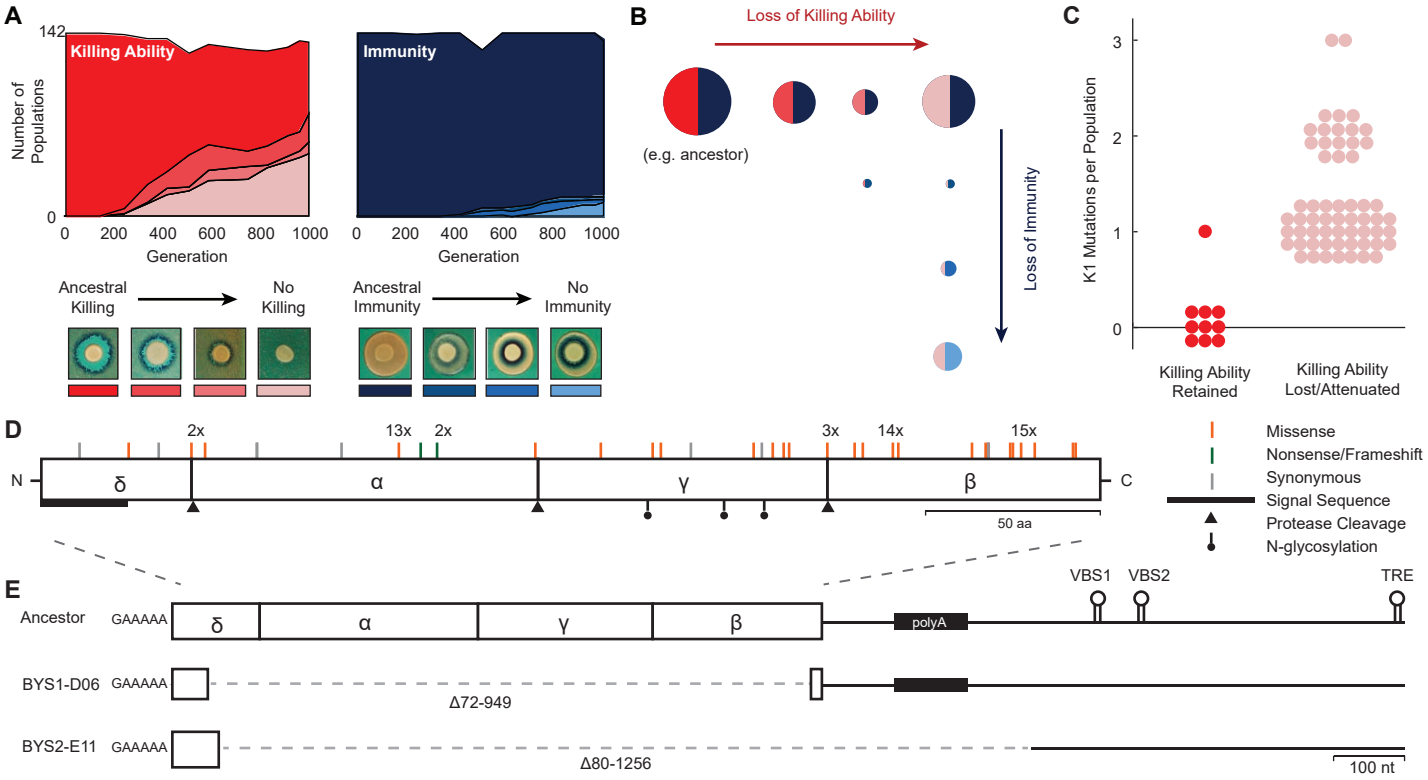

Fig. 2. Widespread loss of killer phenotype correlates with appearance of mutations in the K1 toxin gene. A) Loss of killing ability (left) and immunity (right) from evolving yeast populations over time. Killer phenotypes were monitored by halo assay (bottom). B) Killer phenotype of populations at Generation 1000. Data point size corresponds to number of populations. Color and shade indicate killer phenotype as in panel A. C) Number of mutations in the K1 gene in yeast populations that retain or lose killing ability. Each data point represents a single yeast population. D) Observed spectrum of mutations across the K1 toxin in 67 evolved yeast populations. Mutations were detected in a single population unless otherwise noted. E) Large internal deletion variants from two yeast populations. Deletion indicated by dashed gray line. VBS: viral binding site. TRE: terminal recognition element.

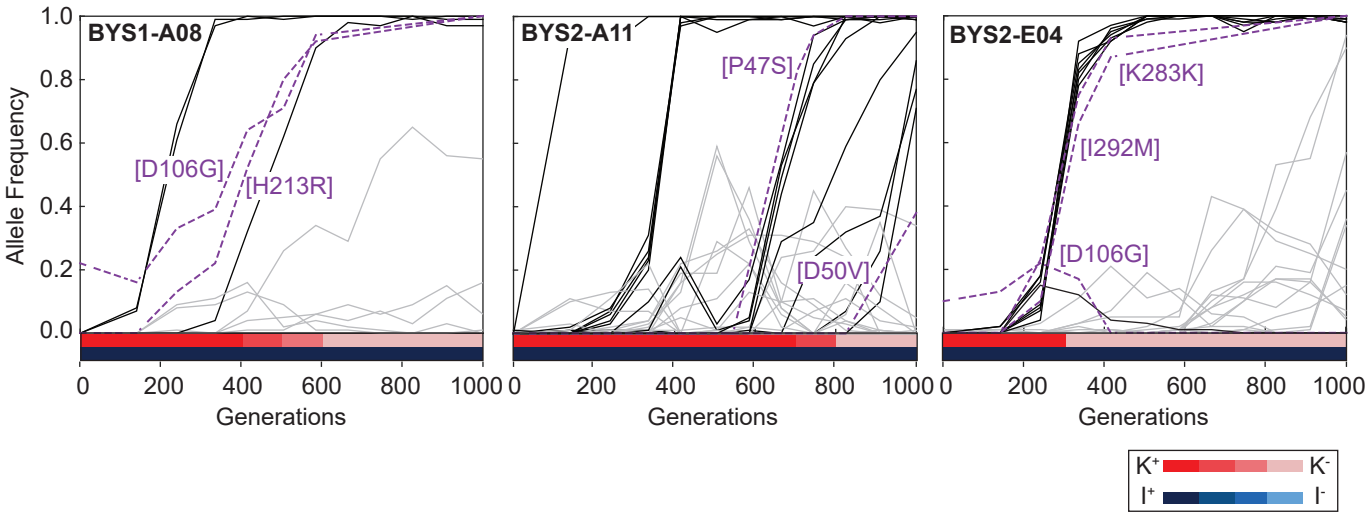

Fig. 3. Viral dynamics mimic nuclear dynamics. Killer phenotype of evolved populations is indicated by color according to the key. Nuclear dynamics (reported previously Lang et al 2014) are represented as solid lines. Nuclear mutations that sweep before or during the loss of killing ability are indicated by black lines. All other mutations are indicated by gray lines. Viral mutations are indicated by purple dashed lines and labeled by amino acid change.

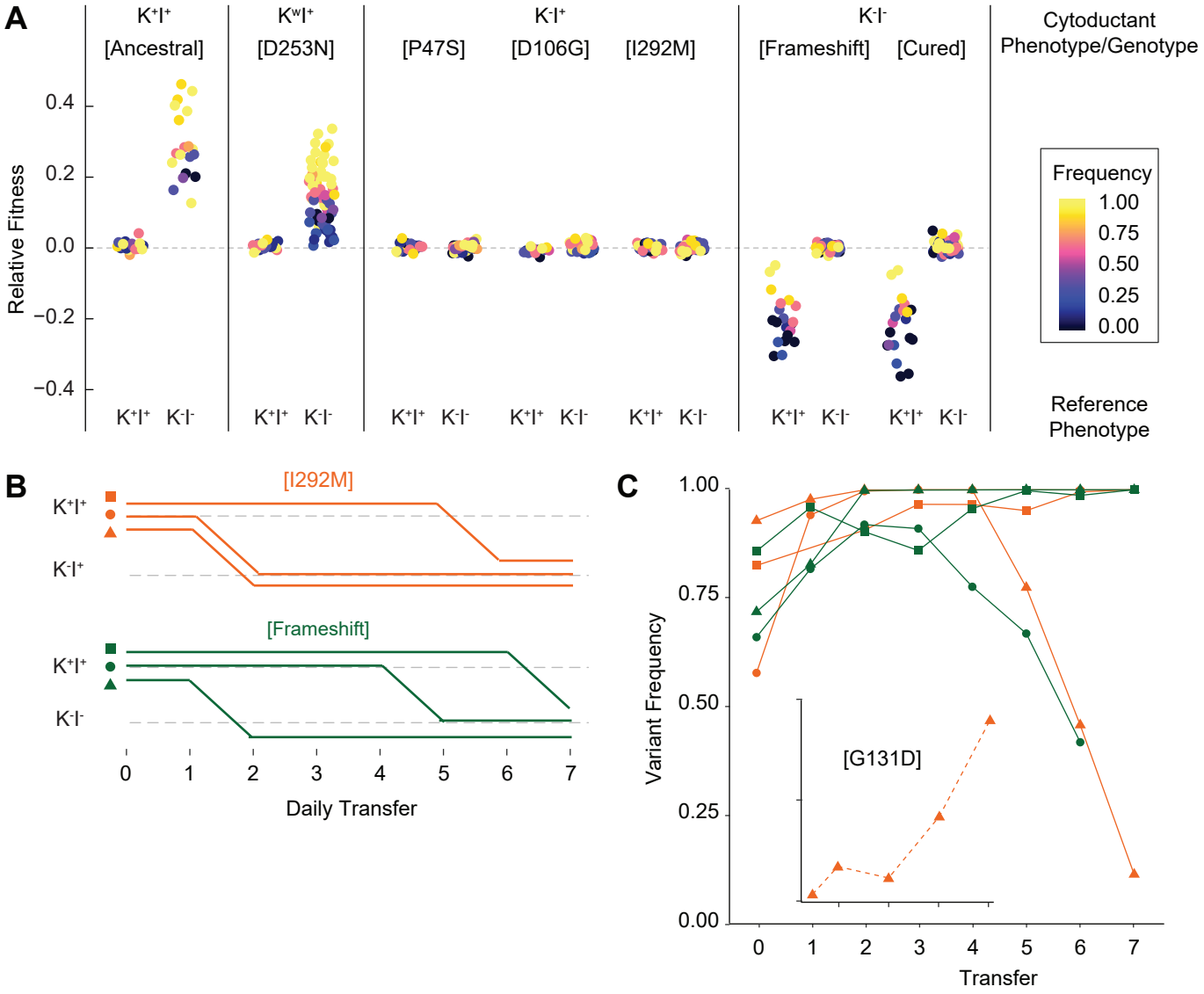

Fig. 4. Viral evolution is driven by selection for an intracellular competitive advantage. A) Relative fitness of viral variants in pairwise competition with the ancestor (K^+I^+) and virus-cured ancestor (K^-I^-). Killer phenotype and identity of viral variant labeled above (K^w indicates weak killing ability). Killer phenotype of the ancestral competitor labeled below. Starting frequency indicated by color. B) Change to killer phenotype during intracellular competitions between viral variants (by color) and ancestral virus. Replicate lines indicated by symbol. C) Variant frequency during intracellular competitions. Colors and symbols consistent with panel B. Inset: frequency of the de novo G131D viral variant.